

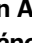

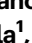



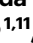






Generation of chimeric antigen receptor T cells targeting p95HER2 in solid tumors

Received: 4 December 2023

Accepted: 8 October 2024

Published online: 18 November 2024

 Check for updates

Macarena Román Alonso ^{1,2,3}, Ariadna Grinyó-Escuer ^{1,2,3}, Santiago Duro-Sánchez ^{1,2,3,4}, Irene Rius-Ruiz¹, Marta Bort-Brusca^{4,5}, Marta Escorihuela¹, Susana Maqueda-Marcos¹, Sandra Pérez-Ramos ¹, Judit Gago ^{1,4}, Vanesa Nogales⁴, Martín Espinosa-Bravo ⁶, Vicente Peg⁷, Santiago Escrivá-de-Romani⁸, Laia Foradada⁹, Laura Soucek ^{1,3,10}, Irene Braña⁸, Vladimir Galvao⁸, Silvia Martín-Lluesma ^{1,11}, Ekkehard Moessner¹², Christian Klein ¹², Elena Garralda ⁸, Cristina Saura ⁸ & Joaquín Arribas ^{1,2,4,5,10} 

The redirection of T lymphocytes against tumor-associated or tumor-specific antigens, using bispecific antibodies or chimeric antigen receptors (CAR), has shown therapeutic success against certain hematological malignancies. However, this strategy has not been effective against solid tumors. Here, we describe the development of CAR T cells targeting p95HER2, a tumor-specific antigen found in HER2-amplified solid tumors. These CAR T cells display robust activity against p95HER2-expressing cell lines but demonstrate limited efficacy against patient-derived xenografts. As p95HER2 is invariably detectable on tumor cells that overexpress HER2, but not those that express HER2 at normal levels, we arm p95HER2-specific CAR T cells with affinity-tuned bispecific antibodies against HER2 and CD3 in order to redirect them only to HER2-amplified cells. The combination of p95HER2.CAR T cells and HER2 x CD3 bispecific antibodies lead to a complete regression in three HER2-positive, patient-derived mouse xenografts tumor models. This combination represents a promising strategy to redirect T cells against a subset of HER2-positive tumors.

Redirection of T lymphocytes against tumor-associated or tumor-specific antigens is a successful therapeutic strategy against certain hematologic malignancies. However, so far, most attempts against solid tumors have failed. T cells can be redirected against cancer cells

using bispecific antibodies of various formats such as bispecific T cell engagers (BiTEs®) or T cell bispecific antibodies (TCBs). These bispecific antibodies simultaneously bind the tumor antigen and an invariant subunit of the T cell receptor (TCR), typically CD3¹. An alternative

¹Vall d'Hebron Institute of Oncology (VHIO), Vall d'Hebron Barcelona Hospital Campus, Barcelona 08035, Spain. ²Centro de Investigación Biomédica en Red de Cáncer (CIBERONC), Monforte de Lemos, Madrid 28029, Spain. ³Department of Biochemistry and Molecular Biology, Universitat Autònoma de Barcelona, Bellaterra 08193, Spain. ⁴Cancer Research Program, Hospital del Mar Research Institute, Barcelona 08003, Spain. ⁵Department of Medicine and Life Sciences, Universitat Pompeu Fabra, Barcelona 08002, Spain. ⁶Breast Surgical Unit, Breast Cancer Center, Gynecology Department, Vall d'Hebron University Hospital, Barcelona 08035, Spain. ⁷Surgical Pathology, Anatomical Pathology, Clinical Laboratories, Vall d'Hebron University Hospital, Barcelona 08035, Spain. ⁸Medical Oncology Service, Vall d'Hebron Barcelona Hospital Campus, Vall d'Hebron Institute of Oncology (VHIO), Barcelona 08035, Spain. ⁹Peptomyc S.L., Barcelona 08035, Spain. ¹⁰Institució Catalana de Recerca i Estudis Avançats (ICREA), Barcelona 08010, Spain. ¹¹Departamento de Ciencias Médicas Básicas, Facultad de Medicina, Universidad San Pablo-CEU, CEU Universities, Madrid 28668, Spain. ¹²Roche Innovation Center Zurich, Roche Pharma Research and Early Development, Schlieren 8952, Switzerland. ✉ e-mail: jarribas@researchmar.net

strategy is the transduction of T cells to express chimeric antigen receptors (CARs), which are engineered proteins that combine the antigen-binding domain of an antibody with the signaling domains from the CD3 subunit of the TCR and co-stimulatory receptors such as CD28 or 4-1BB².

Given the scarcity of tumor-specific antigens, most bispecific antibodies and CAR T cells developed to date have been directed against tumor-associated antigens. These are often expressed in normal tissues and, consequently, serious side effects caused by on-target off-tumor activity have limited the use of bispecific antibodies and CARs³.

The gene encoding the tyrosine kinase receptor HER2 is amplified in ~4% of all tumors. In some tumors, such as those affecting the breast and the upper gastrointestinal tract, the frequency of HER2 amplification reaches ~15%. More than one third of these tumors also express a truncated form of HER2, known as p95HER2⁴. Compared to breast cancers expressing only full-length HER2, those expressing p95HER2 are more aggressive and resistant to trastuzumab, a therapeutic anti-HER2 antibody, as monotherapy⁵. However, p95HER2-positive breast cancers are sensitive to the combination of trastuzumab and chemotherapy⁶. Several groups, including ours, have independently developed antibodies against epitopes exposed in p95HER2 but inaccessible in full-length HER2^{7–9}. Using these specific antibodies, we showed that, in contrast to HER2, which is expressed in normal tissues of epithelial and mesenchymal origin, p95HER2 is a bona fide tumor-specific antigen¹⁰. Therefore, redirection of T cells via p95HER2 should be effective on HER2-positive tumors that express p95HER2, and it is expected to lack on-target off-tumor toxicity. Confirming this notion, we have shown that a p95HER2 TCB has activity, albeit limited, against p95HER2-positive breast tumors, while it has no effect on a variety of normal cells expressing physiological levels of HER2¹⁰.

Because of the therapeutic failures on solid tumors, efforts have focused on refining strategies to redirect T cells. While improvement in the design of TCBs has inherent limitations, CAR T cells can be used as platforms to deliver additional anti-tumor factors such as cytokines or antibodies³. For example, T cells engineered to express CARs against the tumor-specific antigen EGFRvIII and, simultaneously, bispecific antibodies targeting EGFR have been shown to be efficacious against experimental models of human glioblastoma¹¹.

Here, we present the development of CAR T cells targeting p95HER2. Characterization of these p95HER2.CAR T cells showed that they have a long-lasting anti-tumor effect on cell lines expressing p95HER2, grown as primary tumors or as metastases. In contrast, p95HER2.CAR T cells have a limited effect against breast cancer patient-derived xenografts (PDXs), an experimental model closer to real tumors than established cell lines. To increase efficacy, we generated T cells expressing bispecific antibodies directed against CD3 and HER2. The affinity of these antibodies against HER2 was tuned down to avoid binding to cells expressing normal levels of HER2. As did p95HER2.CARs, these affinity-tuned bispecific antibodies had limited effect on PDXs. However, the combination of the activity of p95HER2.CAR and affinity tuned anti-HER2 antibodies produced durable complete responses in the majority of PDXs tested. Further, these next generation CAR T cells were effective against cell lines derived from HER2-positive tumors of the upper gastrointestinal tract.

In summary, T cells constitute an expandable platform that can express different therapeutic factors, such as p95HER2.CAR and HER2 x CD3 bispecific antibodies. The combined action of these factors, which target different tumor-specific antigens show a remarkable activity on different experimental models driven by HER2. These findings pave the way for a new treatment for tumors driven by HER2, which represent a 4% of all tumors.

Results

Generation and characterization of p95HER2.CAR T cells

The workflow to generate CAR T cells targeting p95HER2 is represented in Fig. 1A. Briefly, out of eight murine anti-p95HER2 monoclonal antibodies, we selected three because they stained cells expressing p95HER2 more intensely (Supplementary Fig. S1A). The epitopes recognized by these anti-p95HER2 antibodies were similar, but not identical; while the optimal epitope recognized by 14D and 15C antibodies was PIWKFPDE, the epitope optimally recognized by 32H was one amino acid shorter. The corresponding mouse sequence (PIW-KYPDE) was not recognized by any of the anti-p95HER2 antibodies (Supplementary Fig. S1B and ¹⁰).

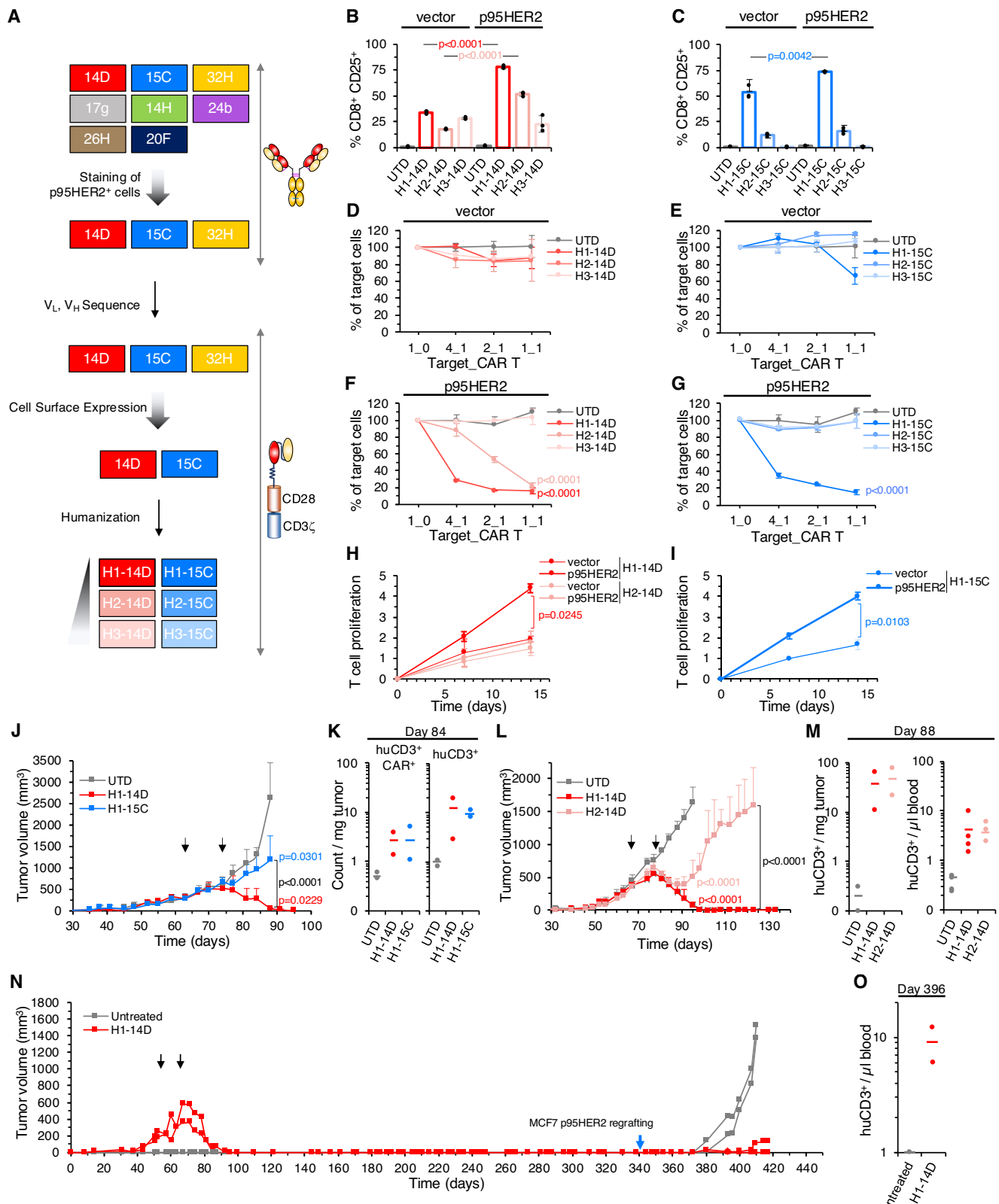
The sequences of the variable regions of the heavy and light chains of these antibodies were used to construct the scFv (single-chain variable fragment) regions of second-generation CARs containing CD28 and CD3 ζ signaling domains. Only two of these CARs were expressed at the cell surface of T cells (Supplementary Fig. S1C). Accordingly, only these two CARs exhibited cytotoxic activity against target cells (MCF7 cells, derived from a non-HER2-amplified breast tumor) transfected with p95HER2 (Supplementary Fig. S1D).

The sequences of the murine scFv regions of these CARs were humanized to various degrees. With the resulting sequences, we generated six humanized p95HER2.CAR T cells. Note that all the versions of the 14D CAR have the same variable light chain. The light and heavy chains corresponding to 15C were combined as indicated (Supplementary Fig. S1E).

The six humanized p95HER2.CAR T cells were characterized by co-culturing them with MCF7 cells transfected with empty vector or p95HER2. The efficiency of transduction of the different CARs ranged from 25–75%; as an illustrative example, in Supplementary Fig. S1F, we show the efficiencies of transduction of the H1-14D CAR and those of additional p95HER2.CAR versions characterized in the next sections. In co-culture with MCF7 p95HER2 cells, CD8-positive cells expressing three of the CARs tested (H1-14D, H2-14D and H1-15C) presented a statistically significant increase in the expression of the activation marker CD25 (Fig. 1B, C). The cytotoxicities induced by the H1-14D and H1-15C CAR T cells on cells expressing p95HER2 were higher than that induced by H2-14D (Fig. 1D–G). We selected the three p95HER2.CAR T cells with detectable levels of activation and cytotoxic ability for in vivo analyses. The H2-14D CAR did not promote T cell proliferation (Fig. 1H), indicating that the extent of activation induced by this CAR is comparatively lower.

The in vivo efficacy of the H1-14D CAR T cells on MCF7 cells expressing p95HER2 was superior to that of H1-15C (Fig. 1J). On day 84, two mice of each group were euthanized, and their tumors processed to analyze the presence of human lymphocytes. As expected, CAR-positive cells were readily detected in tumors from mice treated with H1-14D or H1-15C. Analysis of human CD3-positive cells, that is, T cells, showed a similar distribution, suggesting that among infiltrating CD3 positive cells a sizeable fraction expresses the CAR (Fig. 1K). A similar conclusion was reached when we compared the in vivo effects of H1-14D and H2-14D (Fig. 1L). Again, the infiltration of human CD3-positive cells was much higher in mice treated with CAR T cells. Furthermore, the levels of circulating human lymphocytes followed the same trend (Fig. 1M). In summary, the H1-14D CAR T had a potent anti-tumor effect, superior to those of other CAR T cells.

Long-term monitoring of two mice treated with H1-14D CAR T showed durable responses (Fig. 1N). We used these mice, along with age-matched untreated controls, to investigate whether long-lived p95HER2.CAR T cells protected against tumor cells expressing p95HER2. Thus, after > 350 days, we engrafted again MCF7 p95HER2 cells into the same mice and in the age-matched mice. Remarkably, tumors developed in these control mice but not in the mice previously treated with p95HER2.CAR T cells (Fig. 1N, O). We concluded that mice



treated with p95HER2.CAR T cells remain protected against tumors expressing p95HER2.

Specificity of the p95HER2.CAR and effect on cells expressing normal levels of HER2

To assess the specificity of the selected CAR, H1-14D, first we analyzed the binding of the corresponding scFv to a protein array containing

~6000 native human membrane proteins. As expected, H1-14D scFv did not show significant cross-reaction with full length HER2 (Fig. 2A). The analysis identified two putative cross-reacting proteins (Fig. 2A); the cell surface receptor IL2RB and the transmembrane protein UBXN8, expected to be located primarily at the endoplasmic reticulum¹². To validate these potential hits, we transduced cells with vectors encoding IL2RB and UBXN8 tagged at the cytoplasmic

Fig. 1 | Generation and characterization of p95HER2.CAR T cells. **A** Schematic of the workflow used to generate p95HER2.CARs. **B, C** MCF7 cells expressing empty vector or the same vector encoding p95HER2 were co-cultured with CAR T cells at a 2:1 ratio for 48 h. The percentages of activated CD8⁺ cells (CD8⁺CD25⁺) were determined by flow cytometry. Results are expressed as averages \pm SD of three independent experiments, each using lymphocytes from a different healthy donor. Example histograms for each group are shown in Supplementary Fig. S5. **D–G** The same cells as in (**B, C**) were co-cultured with different ratios of CAR T cells for 48 h. Then, viable target cells were quantified by flow cytometry using EpCAM as a marker, and the percentage of live target cells was calculated by normalizing to the UTD group. Results are expressed as average \pm SD of three independent experiments, each using lymphocytes from a different healthy donor. **H, I** Antigen specific proliferation was determined by co-culturing H1-14D, H2-14D and H1-15C CAR T cells with vector or p95HER2-expressing MCF10A cells and counting lymphocytes at days 0, 7 and 14. Population doublings were calculated relative to initial plating counts. Averages of two independent biological replicates \pm SD, each with a different healthy donor, are shown. **J** 3×10^6 MCF7 cells expressing p95HER2 were injected into the mammary fat pads of NSG mice. At the time points indicated by the black arrows, 3×10^6 T cells transduced with empty vector (UTD) or different p95HER2.CARs (H1-14D or H1-15C) were injected i.v. Results correspond to a single biological replicate using the same donor for all treatment groups. Group tumor volumes are represented as averages \pm SD ($n = 5$). **K** Two mice from each treatment

group were sacrificed at day 88 for tumor infiltration analyses. Tumors were excised, and the numbers of CAR-expressing or total infiltrating human CD3⁺ lymphocytes were quantified and expressed as counts per mg of tumor. Individual data points are displayed, with horizontal bars representing the averages of the two measures. Example histograms for each group are shown in Supplementary Fig. S5. **L, M** The same approach as in (**J, K**) was used to compare the effects of the p95HER2.CARs H1-14D and H2-14D. Results correspond to a single biological replicate using the same donor for all treatment groups ($n = 6$). Example histograms for each group in **K** are shown in Supplementary Fig. S5. **N** Mice ($n = 2$), treated as in (**L**) with H1-14D, were long-term followed up for tumor growth (red lines). As indicated by the blue arrow, 3×10^6 MCF7 cells expressing p95HER2 were regrafted into these mice or, as a control, into untreated age-matched mice. Result corresponds to one biological replicate. **O** The numbers of circulating human lymphocytes from mice in (**N**) were analyzed at day 396 and expressed as number of human CD3⁺ cells per μ l of blood. Individual data points are displayed, with horizontal bars representing the averages of the measures. Example histograms for each group are shown in Supplementary Fig. S5. *P*-values were determined using a two-tailed Student's *t*-test for MCF7 vs. MCF7 p95HER2 co-culture (**B, C, H, I**), and two-way ANOVA with Bonferroni's multiple testing correction (**D–G, J, L**) for comparisons between each treatment and the UTD group, as well as between different p95HER2.CAR T cell treatments (in black). *P*-values are indicated when significant.

C-terminus with the V5 epitope. Analysis by flow cytometry of permeabilized cells showed the efficient expression of V5-tagged IL2RB and UBXXN8 (Fig. 2B). Similar analysis of transfected cells with antibodies against a luminal domain of UBXXN8 and against the extracellular domain of IL2RB confirmed that, in contrast to IL2RB, UBXXN8 is not exposed at the cells surface (Fig. 2C). Staining with H1-14D scFv showed no specific cell surface signal in cells overexpressing IL2RB or UBXXN8 (Fig. 2D). Accordingly, p95HER2.CAR T cells did not have any effect on cells expressing these transmembrane proteins (Fig. 2E). We concluded that the two only candidate cross-reacting proteins identified in the membrane protein array were false positives, and that the p95HER2 antibody chosen to construct the p95HER2.CAR does not likely cross-react with any human transmembrane protein other than p95HER2.

Next, we compared the efficacies of the H1-14D CAR T, hereafter referred to as p95HER2.CAR T for simplicity, and a trastuzumab-based HER2.CAR T on MCF7 cells in vivo. These cells express levels of HER2 like those expressed by normal epithelial tissues¹³. As shown in Fig. 2F, while the HER2.CAR T efficiently killed MCF7 tumors, the p95HER2.CAR T had no effect. Analysis of circulating human T cells indicated that the majority of proliferating human CD3-positive cells expressed the p95HER2.CAR, indicating that human CD3 is a useful surrogate marker for CAR T cells (Fig. 2G). We concluded that the p95HER2.CAR does not target cells expressing physiological levels of HER2.

Effect of p95HER2.CAR T cells on different cancer models

Next, we tested the efficacy of the p95HER2.CAR T on different tumor models, including models of metastasis and patient-derived xenografts (PDXs). As for metastasis models, we injected MCF7 p95HER2 cells expressing luciferase (MCF7.p95HER2.Luc⁺) into the tail vein of immunosuppressed mice. After one month, we detected cell growth in the lungs, as shown by the increase in bioluminescence (Fig. 3A). Treatment with the p95HER2.CAR T effectively reduced this growth (Fig. 3A). To analyze tumor growth in additional organs, we injected MCF7.p95HER2.Luc⁺ cells intracranially. Soon after the injection, cells proliferated. Again, treatment with the p95HER2.CAR T reduced tumor size (Fig. 3B). We concluded that the p95HER2.CAR T cells could cross the blood brain barrier and kill p95HER2-expressing tumor cells growing in the brain.

PDXs are experimental models closer to human tumors. As expected, p95HER2.CAR T cells had no effect on a HER2-positive and p95HER2-negative PDX; in contrast, it reduced the growth of a

p95HER2-positive PDX (Fig. 3C, D). This antitumor effect was comparable to that previously observed with anti-p95HER2 T cell bispecific antibodies¹⁰, but far more limited than that observed with cell line derived tumors (Fig. 1J, L).

Development of a next generation p95HER2.CAR T

To increase the efficacy of the p95HER2.CAR T cells, we sought for additional therapeutic components. HER2 bispecific antibodies could increase the efficacy of lymphocytes redirected against cells expressing p95HER2, which invariably overexpress HER2⁶. We designated these bispecific antibodies TECH2s (T cell Engagers against CD3 and HER2). Given that trastuzumab-based HER2 T cell bispecific antibodies would likely recognize cells expressing normal levels of HER2, we produced scFvs with attenuated affinities¹⁴. These affinity-tuned antibodies have been shown to discriminate between cells expressing normal levels of HER2 and those overexpressing it¹⁵. Consequently, we generated vectors expressing a TECH2 based on trastuzumab (TECH2Hi), and two variants with decreasing affinity (TECH2Me and TECH2Lo), either alone, or within a bicistronic construct alongside the p95HER2.CAR (Fig. 4A).

To preliminary characterize these constructs and to show the correct production of the TECH2s by the bicistronic constructs, we used HEK293T cells. Validating the constructs, we detected specific bands corresponding to the expected molecular weight (53 kDa) in the media conditioned by cells transfected with vectors encoding TECH2Hi, TECH2Me or p95HER2.CAR-TECH2Me (Supplementary Fig. S2A). Next, we stained different cells with purified TECH2Hi and Me. The TECH2Hi stained different cells expressing normal levels of HER2; namely, MCF7 cells, human cardiomyocytes, which can be targeted by anti-HER2 therapies, and MC10A, which are derived from normal epithelium. In contrast, we did not detect binding of the TECH2Me to any of these cells (Supplementary Fig. S2B–D). However, TECH2Me did bind to MC10A cells overexpressing HER2 (Supplementary Fig. S2E). As expected, both TECH2Hi and Me stained human T cells similarly (Supplementary Fig. S2F).

The half-life of bispecific T cell engagers lacking Fc is typically short and, therefore, necessitates continual infusion to reach therapeutic concentrations¹⁶. Accordingly, we estimated the half-life of purified TECH2Me in approximately 13 minutes (Supplementary Fig. S2G). Considering this limitation, the continuous production of TECH2Me by T cells likely results in the generation of constant TECH2Me and better anti-tumor responses.

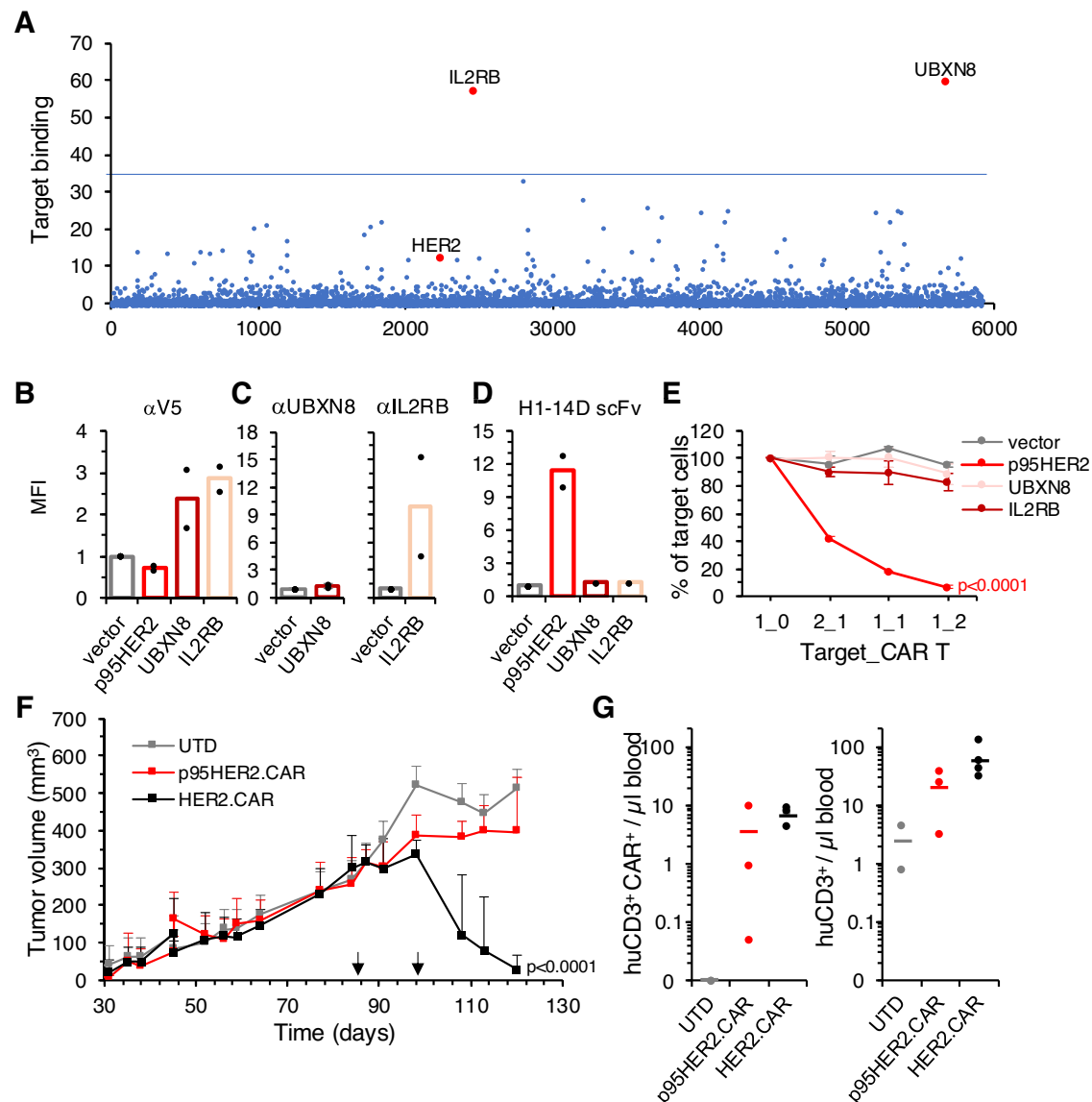


Fig. 2 | Specificity of the p95HER2.CAR T. **A** The scFv of H1-14D was used to stain an array containing ~ 6000 native human membrane proteins. HER2 and two potential positive hits are marked in red. The blue line indicates the binding value above which hits are considered positive. **B–D** MCF10A cells were transduced with empty vector or the vectors encoding p95HER2, UBXN8 or IL2RB, the latter two tagged with the V5 epitope. These cells were stained with anti-V5 antibodies (**B**), antibodies against UBXN8 or IL2RB (**C**) or the scFv of H1-14D (**D**). Individual data points and bars representing the averages of two independent determinations normalized to MCF10A-vector are represented. MFI: mean fluorescence intensity. Example histograms for each group are shown in Supplementary Fig. S5. **E** The same cells as in **B** were co-cultured with p95HER2.CAR T cells for 48 h. Then, viable target cells were quantified by flow cytometry using CD3 as a negative selection marker. Results are expressed as average \pm SD of three independent experiments,

each with a different healthy donor for lymphocytes. P -values comparing with UTD analyzed using two-way ANOVA with Bonferroni's correction are indicated when significant. **F** 3×10^6 MCF7 cells were injected into the mammary fat pads of NSG mice. At the time points indicated by the black arrows, 3×10^6 T cells transduced with empty vector (UTD), p95HER2.CAR (H1-14D) or a trastuzumab-based HER2.CAR were injected i.v. Result corresponds to a single biological replicate and all lymphocytes were obtained from the same donor. Tumor volumes are represented as averages \pm SD ($n = 5$). P -values were determined using two-way ANOVA with Bonferroni's multiple testing correction and are indicated when significant, comparing each treatment group with UTD. **G** At the end of the experiment, the numbers of circulating CAR⁺ and total human CD3⁺ lymphocytes were analyzed and expressed as counts per μ l of blood. Example histograms for each group are shown in Supplementary Fig. S5.

To assess the functionality of the TECH2s, we co-cultured transduced T cells with control MCF7 cells or cells from a HER2-positive PDX (PDX433). T cells expressing the TECH2Hi readily killed MCF7 cells (Fig. 4B), arguing that this bispecific antibody targets cell expressing normal levels of HER2. In contrast, T cells expressing TECH2Me or Lo had no effect on MCF7 cells (Fig. 4B). Similar results were observed with MCF10A cells (Supplementary Fig. S3A, left). Further analyses showed that the TECH2Me was effective on cells from the HER2-amplified PDX433 or MCF10A cells overexpressing HER2 (Fig. 4C and Supplementary Fig. S3B, left). The TECH2Lo was unable to effectively

target the PDX433 (Fig. 4C) and was excluded from further development. These results corroborate that TECH2Me discriminates between cells expressing normal levels of HER2 and cells overexpressing it. Thus, the addition of TECH2Me to the p95HER2.CAR is expected to increase anti-tumor efficacy without compromising safety. Supporting this conclusion, T cells expressing p95HER2.CAR and TECH2Me had no effect on parental MCF7 or MCF10A cells (Fig. 4D and Supplementary Fig. S3A, right) but were active on PDX433 and MCF10A HER2 cells (Fig. 4E and Supplementary Fig. S3B, right). Furthermore, HER2.CAR T cells targeted cardiomyocytes, as did T cells expressing

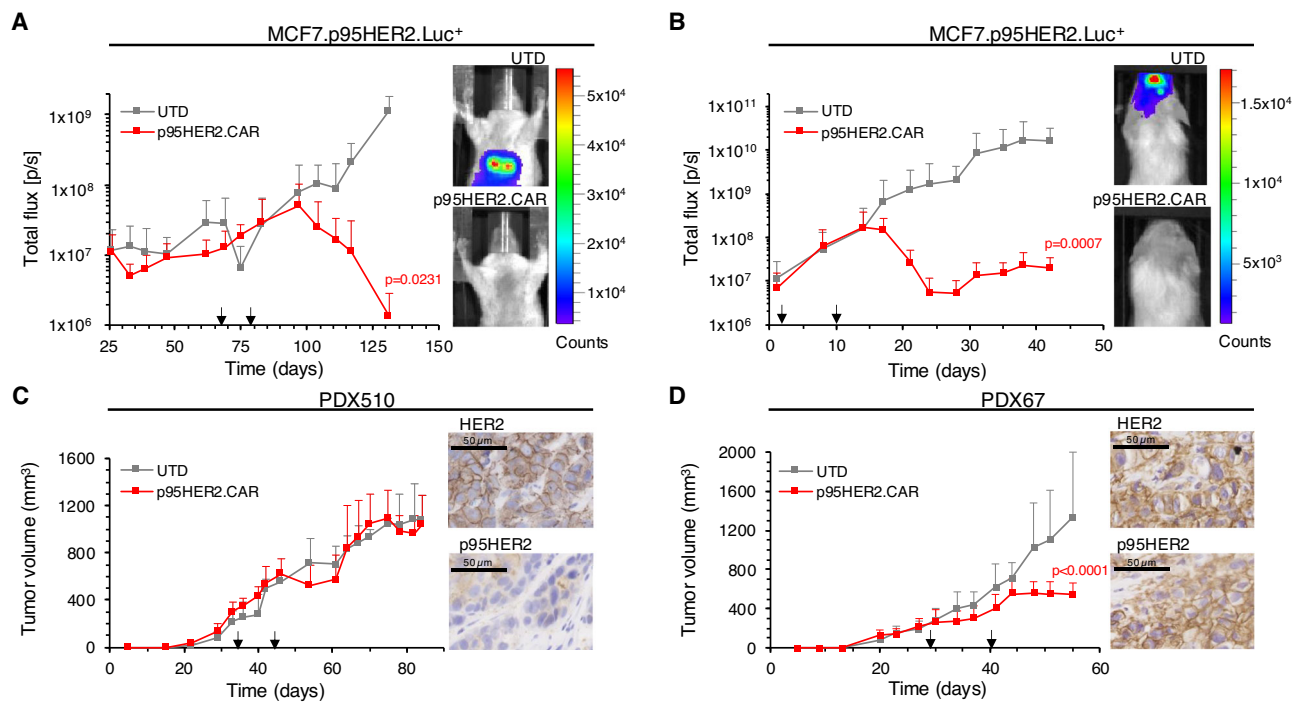


Fig. 3 | Effect of p95HER2.CAR T cells on lung and brain metastases and on PDX models. **A** Left, 1×10^6 MCF7 p95HER2 cells expressing luciferase (MCF7.p95HER2.Luc⁺) were injected into the tail vein of NSG mice. Twenty-five days after the injection, lung metastases were detected by in vivo bioluminescence. At the time points indicated by the black arrows, 3×10^6 T cells transduced with empty vector (UTD) or the p95HER2.CAR were injected i.v. and metastatic growth was monitored and expressed as average \pm SD ($n = 3$). Bioluminescence expressed in total flux measured in photons/second (p/s). Right, representative examples of mice in each group. **B** The same cells as in **A** were injected intracranially (5×10^5 cells) into NSG mice which were treated and monitored as in **A** ($n = 6$). **C** Right, the

indicated PDX was grown in NSG mice. At the time points indicated by the black arrows, 3×10^6 T cells transduced with empty vector (UTD) or p95HER2.CAR T cells were injected i.v. Tumor volumes are represented as averages \pm SD (UTD: $n = 5$; p95HER2.CAR: $n = 7$). Left, Immunohistochemical analysis of HER2 and p95HER2 expression on samples from the same PDXs. **D** The indicated PDX was analyzed as in **C** (UTD: $n = 7$; p95HER2.CAR: $n = 8$). All experiments correspond to a single biological replicate and all lymphocytes within the same experiment were obtained from the same donor. *P*-values were determined using two-way ANOVA with Bonferroni's correction and are indicated when significant, comparing p95HER2.CAR T cell treatment with UTD control group.

p95HER2.CAR-TECH2Hi. In contrast, and supporting their safety, T cells expressing p95HER2.CAR-TECH2Me had no effect (Supplementary Fig. S3C). Finally, we showed that p95HER2.CAR-TECH2Me T cells did not kill additional non-transformed cell lines that express normal levels of HER2 (Supplementary Fig. S3D, E).

Conceivably, part of the TECH2s remain bound to transduced T cells and part is secreted and could bind non-transduced T cells. Indeed, analysis of the media conditioned by human lymphocytes transduced with the p95HER2.CAR-TECH2Me showed the accumulation of soluble TECH2Me (Supplementary Fig. S3F). To test the functionality of secreted TECH2Me, we analyzed the activation of T cells transduced with vectors encoding p95HER2.CAR-TECH2Me or TECH2Hi, co-cultured with PDX433 cells, and we showed the activation not only of transduced, but also of non-transduced T cells (Fig. 4F). Confirming the lack of activity of TECH2Me on cells expressing normal levels of HER2, we did not observe activation of T cells transduced with p95HER2.CAR-TECH2Me, or bystander activation, in the presence of MCF7 cells (Fig. 4F).

These in vitro results were confirmed in vivo; T cells expressing TECH2Hi, alone or in combination with p95HER2.CAR, efficiently killed MCF7 cells (Fig. 4G). Whereas T cells expressing TECH2Me, alone or in combination with p95HER2.CAR, did not kill the same cells (Fig. 4H).

To directly compare the safety and efficacy of the medium affinity scFv expressed as TECH2Me or as CAR, we constructed the latter (Supplementary Fig. S3G). In vitro analysis showed activity of HER2-Me.CAR T cells on MCF7 cells (Supplementary Fig. S3H). This killing activity of T cells expressing the HER2Me.CAR on cells expressing

normal levels of HER2 contrast with the lack of effect of the TECH2Me (Fig. 4B and Fig. 4H). This difference is likely due to a more potent signaling transduced by the HER2Me.CAR, which results in an increase in the number of activated T cells (Supplementary Fig. S3I). Despite this difference on MCF7 cells, both constructs were similarly effective on a p95HER2- and HER2-positive PDX in vivo (Supplementary Fig. S3J). Thus, we concluded that the use of HER2Me.CAR T cells does not increase efficacy but likely compromises safety.

In summary, T cells expressing p95HER2.CAR and TECH2Me do not have any effect on different cells expressing normal levels of HER2. We concluded that this next generation CAR T will likely have very limited side effects in patients.

Anti-tumor efficacy of p95HER2.CAR-TECH2Me T cells

To further assess the efficacy of p95HER2.CAR-TECH2Me T cells in vivo, we used different HER2- and p95HER2-positive breast cancer PDXs (Supplementary Fig. S4A-C). PDX67, which is partially resistant to p95HER2.CAR T cells (Fig. 3D), showed sensitivity, albeit limited, to T cells expressing TECH2Me (Fig. 5A). However, the combined effects of p95HER2.CAR and TECH2Me led to a remarkable effect (Fig. 5A). Long-term monitoring of these mice showed that two had a complete response, and two relapsed (Supplementary Fig. S4D). The treatment did not significantly affect the health of mice as judged by their weights (Supplementary Fig. S4E). The effect of p95HER2.CAR-TECH2Me T cells on two additional PDXs was similar. In one of them, PDX667, we observed partial effects of T cells expressing p95HER2.CAR or TECH2Me, but their combination resulted in complete responses in all treated mice (Fig. 5B and Supplementary Fig. S4F) with

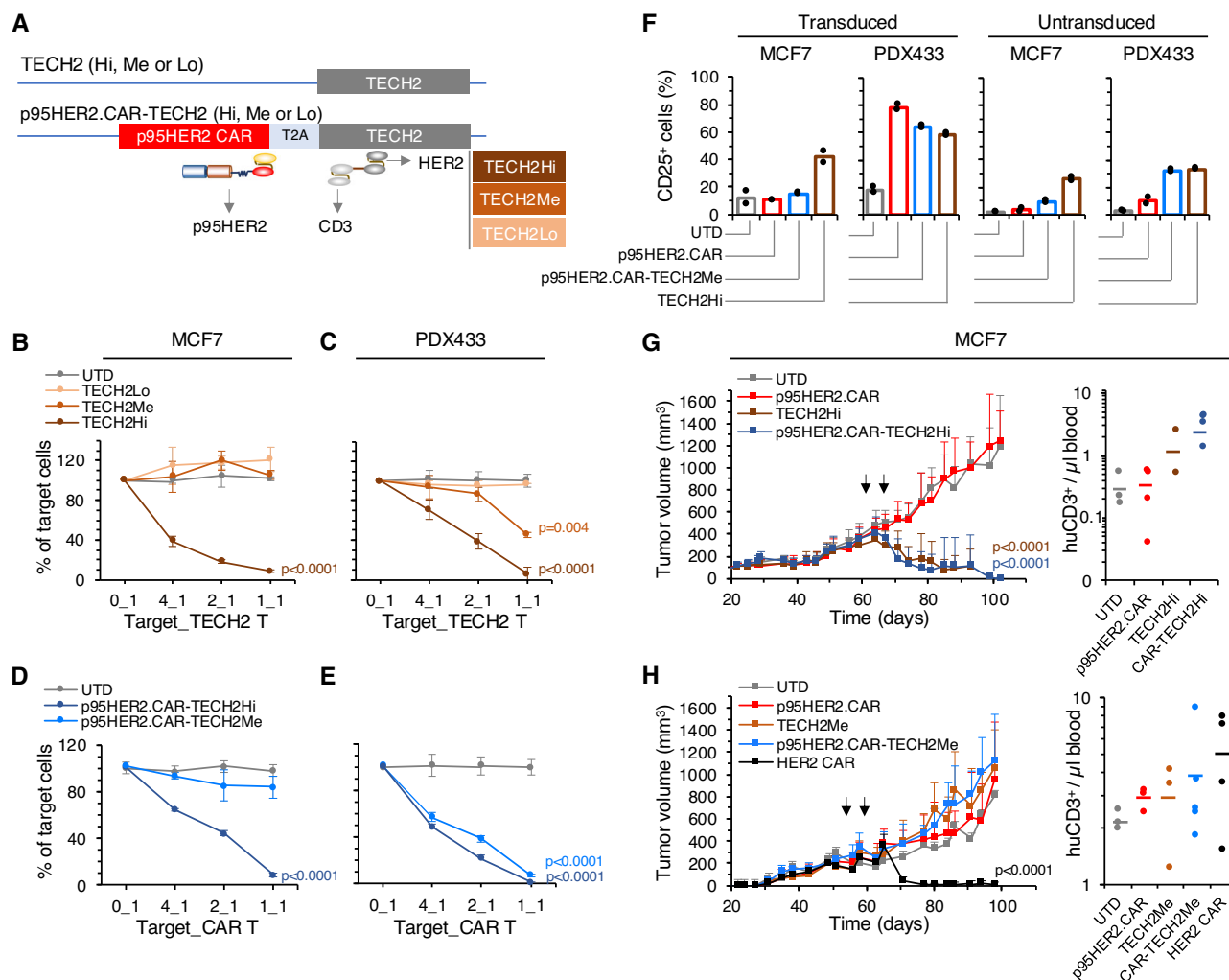


Fig. 4 | Generation and characterization of T cells expressing p95HER2.CARs and TECH2s (T cell Engager against CD3 and HER2) of different affinities.

A Schematic showing the different vectors used. The upper vectors encode TECH2s of different affinities: High (Hi), Medium (Me) or Low (Lo). The lower vectors encode a bicistronic protein consisting of the p95HER2.CAR and the different TECH2s separated by a T2A self-cleaving peptide. **B–E** Parental MCF7 cells or cells from the HER2⁺ and p95HER2⁺ PDX433 were co-cultured with T cells expressing the different TECH2s (**B–C**) or expressing p95HER2.CAR and the indicated TECH2s (**D–E**), at different ratios. Then, viable target cells were quantified by flow cytometry using EpCAM as a marker. Results are expressed as averages of three independent experiments, each with a different healthy donor for lymphocytes, \pm SD. *P*-values were determined using two-way ANOVA with Bonferroni's multiple testing correction and are indicated when significant, comparing each group with the UTD. **F** T cells transduced with the indicated vectors were co-cultured with MCF7 cells or cells from the PDX433. Then, the levels of the activation marker CD25 were

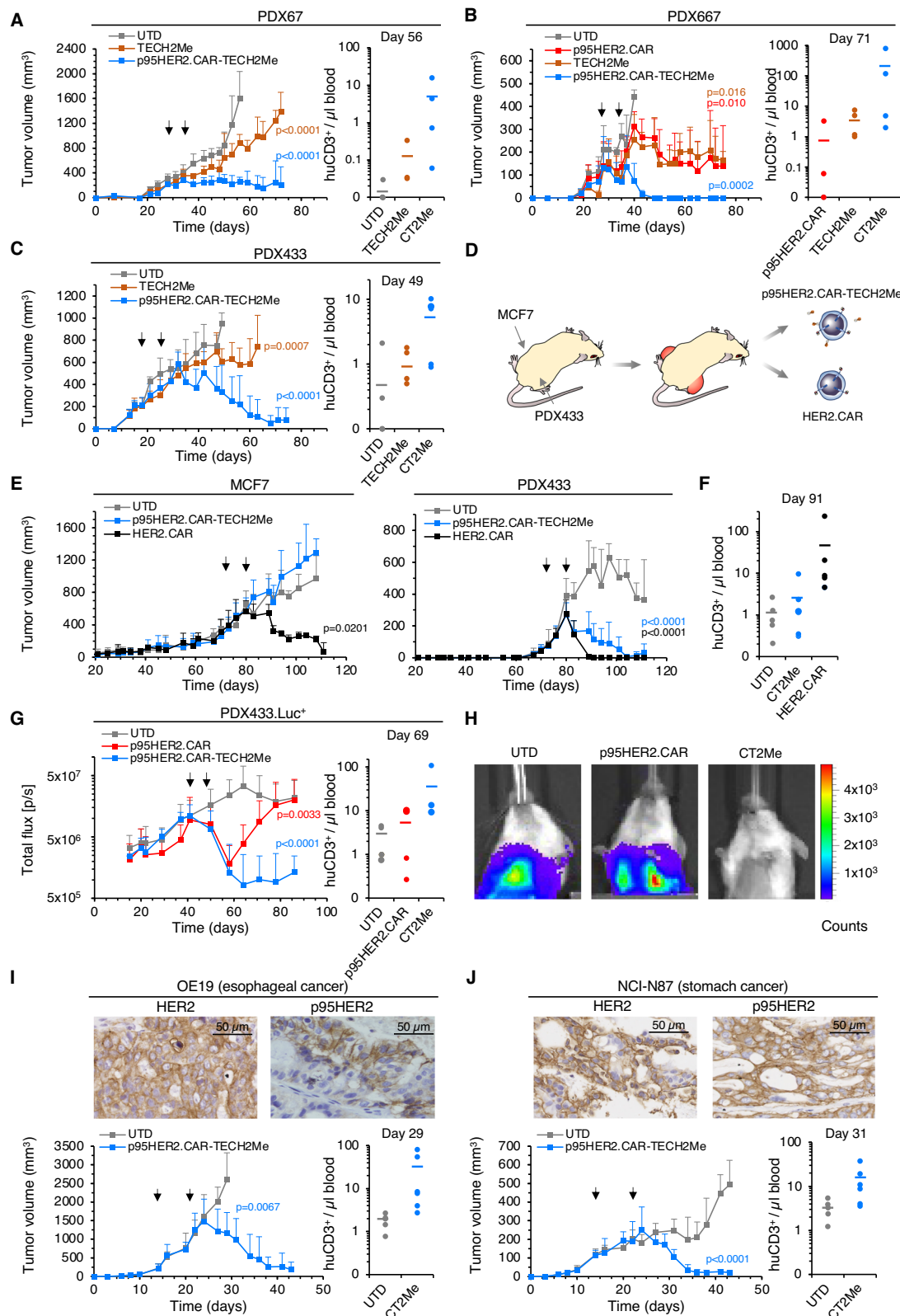
determined in transduced or untransduced CD3⁺ T cells. Individual datapoints and bars representing the average of duplicate determinations are shown, each using a different PBMC donor. Example histograms for each group are shown in Supplementary Fig. S5. **G, H** 3×10^6 MCF7 cells were engrafted into the mammary fat pads of NSG mice. At the time points indicated by the black arrows, 3×10^6 T cells expressing control vector (UTD) or the indicated constructs were injected i.v. All lymphocytes were obtained from the same donor. Tumor volumes are represented as averages \pm SD (In **G**, $n = 7$ except $n = 3$ for TECH2Hi; In **H**, $n = 3$ for UTD and p95HER2.CAR, $n = 4$ for TECH2Me and HER2.CAR, and $n = 5$ for p95HER2.CAR-TECH2Me). At the end of the experiment, the numbers of human lymphocytes were analyzed and expressed as number of CD3⁺ cells per μ l of blood. Example histograms for each group are shown in Supplementary Fig. S5. *P*-values were determined using two-way ANOVA with Bonferroni's multiple testing correction and are indicated when significant comparing each treatment group with the UTD. CAR-TECH2 = p95HER2.CAR-TECH2.

no obvious adverse effects (Supplementary Fig. S4G). In the third PDX, PDX433, we observed complete responses in 3 out of 5 mice (Fig. 5C and Supplementary Fig. S4H), again with no adverse effects (Supplementary Fig. S4I). Thus, in the three PDXs tested, p95HER2.CAR-TECH2Me T cells had a remarkable anti-tumor activity and in most cases the responses were complete.

To support that p95HER2.CAR-TECH2Me T cells target HER2-amplified p95HER2 positive tumor cells but not cells expressing normal levels of HER2, we engrafted MCF7 and PDX433 cells, in opposite mammary glands. Once both types of tumors reached a readily detectable volume, we treated mice with control T cells transduced with empty vector, T cells expressing p95HER2.CAR-TECH2Me or, as a control, with T cells expressing the HER2.CAR (Fig. 5D). As expected,

HER2.CAR T cells efficiently killed both types of tumors. In contrast, T cells expressing p95HER2.CAR-TECH2Me did not have any effect on MCF7 tumors even in mice in which tumors generated by the p95HER2- and HER2-positive PDX responded (Fig. 5E, F).

The p95HER2.CAR-TECH2Me T was also far more effective than the p95HER2.CAR T on lung tumors caused by cells from the p95HER2- and HER2-positive PDX433 expressing luciferase (Fig. 5G, H). Unexpectedly, in these mice we also observed the signal from tumor cells at the site of injection, in the tail vein. These tumors were also efficiently targeted by T cells expressing p95HER2.CAR or p95HER2.CAR-TECH2Me (Supplementary Fig. S4J, K), further supporting the efficacy of these CAR T cells, particularly the latter one, on tumors located in different organs.



The gene encoding HER2 is amplified in ~15% of esophageal and gastric cancers (source, cBioPortal). Several drugs approved to treat HER2-positive breast cancer, such as Lapatinib, T-DM1 or the combination trastuzumab/pertuzumab have not shown efficacy on tumors of the upper gastrointestinal tract^{17–19}. In contrast, p95HER2.CAR-TECH2Me T cells showed remarkable efficacy in xenografts of cell lines derived from HER2-positive esophageal and gastric cancers that

express p95HER2 (Fig. 5I, J). These results indicate that lymphocytes redirected to cells overexpressing HER2 and/or p95HER2 may be efficacious independently of the tumor type.

In summary, our data show that targeting p95HER2 and, in addition, HER2 with medium affinity antibodies, is a safe and efficacious strategy to redirect T cells against p95HER2-positive HER2-amplified tumors.

Fig. 5 | Anti-tumor efficacy and safety of T cells expressing p95HER2.CARs and TECH2s of high and medium affinity. **A–C** The indicated PDXs were engrafted into the mammary fat pads of NSG mice. At the time points indicated by the black arrows, 3×10^6 T cells expressing empty vector (UTD), or the indicated factors were injected i.v. Tumor volumes are represented as averages \pm SD (in A: $n = 5$ for UTD and $n = 4$ for TECH2Me and p95HER2.CAR-TECH2Me; in B: $n = 4$; and in C: $n = 5$). At the end of the experiment, the numbers of human lymphocytes were analyzed and expressed as number of CD3⁺ cells per μ l of blood. **D** Schematic showing the experiment corresponding to panels E and F. MCF7 and PDX433 cells were engrafted into opposite mammary fat pads of NSG mice. When tumors reached ~ 350 and 80 mm^3 respectively, mice were treated with the indicated CAR T cells. **E, F** Mice were treated and analyzed as in A–C (UTD: $n = 5$; p95HER2.CAR-TECH2Me and HER2.CAR: $n = 6$). **G** 1×10^6 cells from PDX433 expressing luciferase were injected in the tail vein of NSG mice. After 2 weeks, growth in lungs was evident by assessing bioluminescence measured in photons per second (p/s) units. Mice were

treated with 3×10^6 T cells expressing empty vector (UTD), or the indicated constructs. All lymphocytes were obtained from the same donor. Results are expressed as means \pm SD ($n = 4$). **H** Representative images taken at the end of the experiment in **(G)**. **I, J** Upper panels, OE19 or NCI-N87 cells were grown as xenografts. Tumors were excised, processed and the levels of HER2 or p95HER2 analyzed by immunohistochemistry with specific antibodies. Lower panels, 5×10^5 OE19 or 1×10^6 NCI-N87 cells, derived from esophageal or stomach cancers respectively, were subcutaneously engrafted into NSG mice. Mice were treated and analyzed as in A–C. Results are expressed as means \pm SD (In, UTD: $n = 5$ and p95HER2.CAR-TECH2Me: $n = 6$; in J: $n = 6$). All results correspond to one biological replicate and all lymphocytes within the same experiment were obtained from the same donor. *P*-values were determined using two-way ANOVA with Bonferroni's multiple testing correction and are indicated when significant, comparing each treatment group with the UTD. Example histograms for each group in **(A–J)** are shown in Supplementary Fig. S5. CT2Me = p95HER2.CAR-TECH2Me.

Discussion

While most HER2-positive breast tumors diagnosed at early stages are currently being successfully treated with surgery combined with neo- and adjuvant precision therapies, advanced tumors still pose an unmet medical need. In addition, although increasingly infrequent, late recurrences of initially responding tumors still occur, and they tend to not be sensitive to currently available anti-HER2 therapies anymore²⁰.

HER2 is arguably the most targeted receptor in the development of cancer therapies. Current approved therapies include therapeutic antibodies, antibody-drug conjugates, and tyrosine kinase inhibitors. The advancement of therapies designed to enhance the immune response against HER2-driven tumors represents a dynamic area of clinical research. These innovative therapies encompass inhibitors of immune checkpoints, agents that activate both innate and adaptive immune responses, and strategies to redirect lymphocytes against HER2, such as bispecific antibodies and chimeric antigen receptor (CAR) T cells²¹.

Further underscoring the need for additional anti-HER2 therapies, other HER2-positive tumors, such as those affecting the gastrointestinal tract, are intrinsically more resistant to current therapies compared to HER2-positive breast tumors^{17–19}. In this context, the redirection of T cells against HER2-positive tumor cells is an attractive therapeutic avenue. One of the difficulties of treating solid tumors with CAR T cells is the on-target off-tumor effects. This hurdle is evident in the case of HER2, which is expressed in many epithelial tumors, albeit at much lower levels than in HER2-amplified tumors. In fact, fatal side effects have been already documented in a patient treated with CAR T cells targeting HER2²².

Since p95HER2 is a bona fide tumor specific antigen, on-target off-tumor effects are not expected, and thus, p95HER2.CAR T cells may be a safe alternative to HER2.CAR T cells. The results shown in this report support this possibility; p95HER2.CAR T cells are effective against p95HER2-expressing cells both in vitro and in vivo but not against cells expressing normal levels of HER2. The anti-tumor activity of the p95HER2.CAR T cells is like that of T cell bispecific antibodies targeting p95HER2¹⁰; both strategies result in clear but partial responses on PDXs. Since engineered T cells are expandable platforms that can be loaded with multiple anti-tumor factors, we added bispecific antibodies (TECH2s) targeting HER2, which is invariably co-expressed with p95HER2. A portion of these TECH2 antibodies remains bound to the T cells that also express p95HER2.CARs, thus arming T cells with a dual mechanism for targeting cancer cells that express p95HER2, which invariably overexpress HER2. Another portion is secreted and binds to T cells that do not express p95HER2.CARs, enhancing the anti-tumor effect through a bystander mechanism that redirects T cells towards cancer cells overexpressing HER2. The combined targeting of anti-p95HER2 and anti-HER2 likely mitigates the emergence of resistance by downmodulation of p95HER2 and/or HER2.

Although preliminary data from two cell lines derived from esophageal and gastric cancers are promising, additional models need to

be examined to fully assess the efficacy of p95HER2.CAR-TECH2Me T cells against these tumors. It is important to note the observed differences between experimental models: while cell lines expressing p95HER2 are responsive to p95HER2.CAR T cells, patient-derived xenografts (PDXs) do not exhibit similar sensitivity. Therefore, to confirm the therapeutic potential of p95HER2.CAR-TECH2Me T cells in gastric tract tumors positive for p95HER2 and/or HER2, further testing across multiple models is required.

To ensure that these bispecific antibodies do not compromise safety by targeting cells expressing physiological levels of HER2, we used previously described versions of the anti-HER2 scFv with attenuated affinities¹⁴. The TECH2Me had no effect on different cell types expressing normal levels of HER2. Compared with a bispecific antibody of higher affinity, the TECH2Me has limited anti-tumor ability, but combined with the p95HER2.CAR, induces the total regression of most tumors tested. Furthermore, these next generation CAR T cells are also effective against different metastases, indicating that they could be therapeutic even in advanced stages.

Unlike therapeutic anti-HER2 antibodies or antibody-drug conjugates, tyrosine kinase inhibitors such as lapatinib, neratinib and tucatinib target both HER2 and p95HER2²¹. Lapatinib has been demonstrated to stabilize HER2 on the surface of HER2-overexpressing cells, leading to increased receptor levels²³. Consequently, lapatinib treatment may enhance the efficacy of CAR T cells engineered to express TECH2Me. Future investigations are required to ascertain whether HER2-inhibitors also modulate the surface levels of p95HER2, which could further inform the potential synergistic application of tyrosine kinase inhibitors in combination with p95HER2-targeted CAR-TECH2Me therapies.

In summary, p95HER2.CAR T cells represent an avenue to achieve complete remissions of a subset of HER2-positive tumors.

Methods

Study design

The overall purpose of this study was to develop a CAR T cell-based approach for the treatment of HER2-amplified tumors. To ensure safety, we used a second-generation CAR targeting p95HER2 and a bispecific antibody that recognizes HER2 with attenuated affinity and CD3 ϵ , an invariant subunit of the TCR. Since p95HER2 is a tumor specific antigen, and the anti-HER2 with attenuated affinity does not bind cells expressing normal levels of HER2, T cells expressing both factors are safe; they do not target cells expressing normal levels of HER2. T cells expressing only p95HER2.CARs or only the bispecific antibody have a limited anti-tumor effect. However, T cells expressing simultaneously both factors are remarkably efficacious against a variety of tumor models.

For in vitro studies, a minimum of two biological replicates were performed. For in vivo experiments, three to seven mice were used per treatment group, and they were randomized by tumor size. All human

samples were obtained following institutional guidelines under protocols approved by the Clinical Research Ethics Committee of Vall d'Hebron University Hospital. Animal work was performed according to protocols approved by the Ethical Committee for the Use of Experimental Animals of the Vall d'Hebron Research Institute. For ethical reasons, we euthanized individual mice or groups when they exhibited observable signs of graft-versus-host disease (such as poor condition, hair loss), when tumor volume exceeded 1700 mm³, or when there was a 20% loss in body weight, as approved by the ethics committee. Euthanasia was performed through cervical dislocation. In vivo experiments were not conducted in a blinded fashion and they were monitored 2–3 times per week.

Cell lines

MCF7 (#HTB-22), MCF10A (#CRL-10317), HEK293T (#CRL-11268), and NCI-N87 (#CRL-5822) were purchased from American Type Culture Collection (ATCC). OE19 (#96071721), were obtained from Sigma-Aldrich. 1BR3.G (#90020507) and HBEC-3KT (#CRL-4051) were obtained from the Hospital del Mar Cancer Cell Line Repository (Barcelona, Spain). GP2-293 cells (#631458) were obtained from Clontech. Cardiomyocytes (iCell® Cardiomyocytes, #01434) were purchased from Cellular Dynamics and cultured according to the supplier's instructions. MCF7 and MCF10A cells expressing p95HER2 or HER2 were generated as described previously¹⁰. Briefly, the MCF7 p95HER2 cell line was generated through lentiviral transduction with two plasmids: a modified pTRIPZ vector (OpenBiosystems-Thermo Fisher Scientific) for p95HER2 overexpression, and a pTRIPZ-shp21 vector (#RHS4430-200281172 clone V3LHS-322234, Open Biosystems-Thermo Scientific), which includes a short hairpin RNA (shRNA) sequence to silence p21, thereby preventing cellular senescence. MCF10A p95HER2 were generated by lentiviral transduction of pLEX-p95HER2, and MCF10A HER2 were generated by retroviral pQCXI-HER2 infection.

Cells were cultured in complete medium (DMEM:F12 (#21331, Gibco) supplemented with 10% fetal bovine serum (FBS) (#10270, Gibco), 1% L-glutamine (#X0550, Biowest) and the corresponding vector resistance antibiotics. MCF10A cells were further supplemented with 1% HEPES (#H0887), 0.5 µg/mL hydrocortisone (#H0888), 20 ng/mL hEGF (#E9644), 100 ng/mL cholera toxin (#C8052), all from Sigma-Aldrich, and 10 µg/mL Insulin (#11376497001, Roche). Cell lines were authenticated by STR profiling at the High Technology Unit of Vall d'Hebron Institute of Research (VHIR-UAT).

Tumor samples and patient-derived tumor xenografts

All tumor samples from patients were collected at Vall d'Hebron University Hospital (Barcelona) following institutional guidelines and approval of the Clinical Research Ethics Committee of Vall d'Hebron University Hospital. Written informed consent was obtained from all patients who provided tissue samples. PDX433 (ER⁺/PR⁺/HER2³⁺) was extracted by core needle biopsy (CNB) from a breast cancer patient's metastasis in the liver. PDX667 (HER2⁺) was extirpated by CNB from a breast cancer patient's metastasis in the skin. PDX67 (ER⁺/PR⁺/HER2³⁺) was extirpated by CNB from a primary breast cancer tumor.

Fragments of patient samples were implanted into the fat pad of NOD-scid IL2Rgamma^{null} (NSG) (#005557, Charles River Laboratories) mice, and 17β-estradiol (1 mM) (#E8875-1G, Sigma-Aldrich) was added to drinking water. Tumor xenografts were measured with calipers three times per week, and tumor volume was determined using the following formula: Tumor volume = (length × width²) × (π/6). PDX433 was set up in culture in complete DMEM:F12 media after tumor growth in NSG mice. Animal studies were approved by the Ethical Committee for the Use of Experimental Animals of the Vall d'Hebron Research Institute in accordance with the Declaration of Helsinki.

p95HER2 antibodies

Murine monoclonal antibodies targeting human p95HER2 were generated using hybridoma technology⁷. Dot blot assay to determine the epitope of the antibodies was performed as follows. Overlapping 8-mer peptides from the extracellular region of human HER2 were immobilized to a nitrocellulose membrane and antibodies were incubated for 30 min. Membranes were developed using peroxidase-linked secondary antibody.

Humanization of the heavy (V_H) and light (V_L) chains of the best two candidates was performed by Roche using proprietary technology. Three humanized versions of each murine antibody were produced, sequenced and tested.

Membrane proteome array

The Membrane Proteome Array (MPA) screening was conducted at Integral Molecular, Inc. (Philadelphia, PA, USA). The MPA is a protein library composed of ~6000 human membrane proteins, each over-expressed in HEK293T cells by individual transfection in separate wells of a 384-well plate. Transfected cells were pooled by columns and rows, so that each protein was represented in two unique wells of a matrix and incubated with an scFV-hlgG1 fusion containing the H1-14D scFv of the CAR (Creative Biolabs; Shirley, NY, US). H1-14D scFv binding to specific targets was identified by detecting fluorescence of a secondary labeled antibody on Intellicyt iQue (Sartorius). Each individual membrane protein target was assigned values corresponding to the binding values of their unique row and column pools, allowing for specific deconvolution, and targets displaying binding of > 3 standard deviations above background in both wells were selected for downstream validation experiments²⁴.

To validate the hits, MCF10A cells were infected with lentivirus to overexpress the proteins using plasmids pLX304-hIL2RB (#HsCD00437471, DNAsu) and pLenti6.3/V5-hUBXN8 (#HsCD00954617, DNAsu), and cells were under blasticidin selection for a week to ensure survival of transduced cells. For detection of the overexpressed proteins, the following antibodies were used, coupled to the appropriate labeled secondary antibody: anti-V5 tag (#R961-25, Invitrogen) and anti-IL2RB (#MAB224, R&D Systems) were coupled with AF488-conjugated anti-mouse IgG (#A11001, Invitrogen), and anti-UBXN8 (#HPA077538, Sigma-Aldrich) was coupled with AF488-conjugated anti-rabbit IgG (#A11008, Invitrogen).

Generation of retroviral vectors containing CAR constructs

All CAR, TECH2 and CAR.TECH2 constructs were synthesized and cloned into the retroviral vector pMSGV1 (kindly provided by Dr. Steven Rosenberg, National Cancer Institute, USA), which includes the murine stem cell virus (MSCV) long-terminal repeat (LTR) promoter (GenScript; Rijswijk, Netherlands). The CAR constructs contain a CD8 hinge domain, a CD28 transmembrane and intracellular co-stimulatory domain, and a CD3ζ signaling domain.

Nine anti-p95HER2.CAR constructs were generated with different scFvs. The complete sequences of the anti-p95HER2 scFvs are described in Supplementary Fig. 1E. HER2.CAR (high affinity) construct generation was previously described²⁵ and the HER2Me.CAR was generated using the same HER2-targeting scFv than that of the TECH2Me. Empty pMSGV1 construct was used for control (UTD). TECH2 constructs are composed by two scFvs against HER2 and CD3 linked by a (G4S)₃ linker. The two scFvs are preceded by an IgK leader sequence, and followed by a T2A and a transgene coding for eGFP to evaluate transduction efficiency of the constructs. The high affinity anti-HER2 scFv is based on 4D5 scFv, the medium affinity on 4D5-5 scFv and the low affinity on 4D5-3 scFv¹⁴. The anti-CD3 scFv was derived from a publicly available sequence for blinatumomab. The p95HER2.CAR-TECH2 constructs have the p95HER2.CAR under the LTR promoter followed by a T2A and the TECH2 sequences without the eGFP. The different p95HER2.CAR and TECH2 construct sequences can be

found in patent families with application numbers EP20382457 and EP22382294.

CAR and TECH2 retroviruses were produced as follows. 7.5×10^6 GP2-293 (#631458, Clontech) cells were seeded in 10 cm culture plates coated with Poly-L-Lysine (#P8920-100ML, Sigma-Aldrich) at 0.001% w/v in $1 \times$ phosphate-buffered saline (PBS). The day after, cells were transfected with 4 μ g of envelope plasmid RD-114 (a gift from Alena Gros' Lab, VHIO) and 9 μ g of transfer plasmid (encoding the different constructs), with 60 μ L of Lipofectamine2000 (#11668-019, Invitrogen). Media was changed after 6–8 h. Cell supernatants containing retrovirus particles were collected 72 h after transfection and filtered before being transduced into T cells.

PBMC isolation

Peripheral blood mononuclear cells (PBMCs) were isolated from fresh buffy coats obtained from healthy donors through the Blood and Tissue Bank of Catalonia (BST). Buffy coats were diluted 1:2 with $1 \times$ PBS, transferred slowly to a 50 ml falcon tube with Ficoll-Paque PLUS (#17-1440-02, GE Healthcare) at a 4:3 ratio, and spun following the manufacturer's instructions. After obtaining the PBMC fraction, red blood cells (RBC) were lysed with $1 \times$ RBC lysis buffer (#00-4333-57, Invitrogen) for 5 min. PBMCs were counted, frozen and stored in liquid nitrogen until used for the transduction of CAR constructs.

CAR T cell production

PBMCs containing T cells, isolated from healthy donor buffy coats as described in the previous section, were activated by adding 300 IU/mL interleukin-2 (IL-2) (Proleukin®, Iovance Biotherapeutics) and anti-CD3/anti-CD28 dynabeads (#11131D, Gibco) at 1:1 ratio in PBMC media, composed by RPMI 1640 (#61870, Gibco), 10% heat-inactivated FBS (#10270, Gibco), 1% L-glutamine (#X0550, Biowest), 1% HEPES (#H0887, Sigma-Aldrich) and 1% penicillin–streptomycin (#P4333, Merck), and cultured for 2 days. Retroviruses corresponding to different CAR constructs were transduced into activated T cells in retromycin-coated plates (#T100A, Takara). Cultures were allowed to expand for 7–10 days in their media supplemented with 300 IU/mL IL-2 (Proleukin®, Iovance Biotherapeutics), at which point they were cryopreserved in Cryostor® CS10 (#7930, StemCell Technologies) and stored in liquid nitrogen until use for in vivo assays. After 3 days in culture, CAR surface expression was detected by flow cytometry on BD FACSCanto II or BD FACSCelesta (BD Bioscience) and analyzed using FlowJo software. Transduced T cells were stained with biotinylated anti-mouse F(ab')₂ antibody (#115-065-072, Jackson ImmunoResearch) followed by streptavidin-APC (#405207, Biolegend) or streptavidin-FITC (#SA1001, Invitrogen).

In vitro cytotoxicity, activation and proliferation assays

CAR T cells were normalized to transduction efficiency for co-culture experiments. 10,000 target cells were seeded in 96-well flat bottom plates and incubated at 37 °C, 5% CO₂ overnight. CAR T cells were added the next day at different ratios of target cell to CAR T cells. Plates were incubated for 48 additional hours. Co-cultures were then harvested with trypsin and resuspended in flow cytometry buffer, consisting in $1 \times$ PBS supplemented with 2.5 mM EDTA, 1% bovine serum albumin (BSA) (#A9647-500G, Sigma-Aldrich), and 5% horse serum (#26050088, Life-technologies), for flow cytometric analysis. Percentage of viable target cells was determined by counting the alive cells on each well and normalizing these counts to wells containing T cells transduced with an empty vector (UTD). Target cells were identified by staining with anti-EpCAM-AF647 (#324212, Biolegend) or by negative selection of T cells using anti-hCD3-PE (#300408, Biolegend). The viability marker Zombie Aqua (#423102, Biolegend) was used.

To identify the percentage of activated (CD25-positive) CD8 T cells in co-culture experiments anti-CD8-PE/Cyanine7 (#344712, Biolegend) and anti-CD25-BV421 (#302630, Biolegend) antibodies

were used. To identify transduced cells or bystander activation of T cells, anti-mouse F(ab')₂ antibody coupled to FITC-streptavidin (#SA1001, Invitrogen) was also added to the wells. Samples were assayed in the LSR Fortessa cytometer (BD Biosciences) and analyzed using FlowJo software.

For antigen stimulation proliferation assays, CAR T cells were co-cultured with MCF10A or MCF10A overexpressing p95HER2 cells at 1:1 ratio of effector:target. CAR T cells were transferred to a new well with freshly seeded MCF10A or MCF10Ap95HER2 cells every 48 h and replated at 1×10^6 CAR T cells/mL of fresh T cell media. For each condition, T cells were counted and analyzed using Vi-CELL™ XR Cell Viability Analyzer (Beckman Coulter) at days 0, 7 and 14 of expansion, and population doublings relative to day 0 were calculated.

In vivo tumor growth assays

4–6 week-old NSG female mice were purchased from Charles River Laboratories (#005557), housed in a specific pathogen-free (SPF) animal facility, and injected with different cell lines or PDXs to generate xenografts at 6–8 week-old. MCF7 p95HER2 cells (3×10^6), PDX433 cells (1×10^6), MCF7 cells (3×10^6) or ~3 mm \times 3 mm tumor fragments of PDX67 or PDX667 were implanted orthotopically into the fourth pad of NSG mice. OE19 cells (5×10^5) and NCI-N87 cells (1×10^6) were implanted subcutaneously. Cell lines were implanted using Matrigel (#356235, Cytel) at a 1:1 ratio of cells in PBS to Matrigel. Beta-estradiol (#E8875, Sigma-Aldrich) was added to drinking water. p95HER2 expression of MCF7 p95HER2 cells was induced with doxycycline (1 g/L) in drinking water. Tumors were measured using calipers twice a week and volume was calculated using the formula: tumor volume = (length \times width²) \times ($\pi/6$). Mouse body weight was monitored once a week.

Once tumors reached 100–300 mm³, mice were randomized into treatment groups with similar tumor volumes and treated intravenously (i.v.) with 3×10^6 CAR-positive T cells twice. Animals from all treatment groups and controls were co-housed and tumor volume monitored twice a week until sacrificed by cervical dislocation. Mice blood and tumors were collected and analyzed at the indicated time-points. The same amount of blood for each mouse was lysed with RBC lysis buffer (#00-4333-57, Invitrogen) twice and blocked with flow cytometry buffer before staining. Tumors were weighted, mechanically disrupted, and enzymatically digested with collagenase (#C2674, Sigma-Aldrich) and hyaluronidase (H3506-1G, Sigma-Aldrich) in PBMC medium for 1 h at 37 °C shaking at 80 rpm. The samples were then filtered through 100 μ m strainers and red blood cells were lysed. Cells were resuspended in flow cytometry buffer and stained for analysis. Anti-hCD3-PE (#300408, Biolegend) and biotinylated anti-mouse F(ab')₂ antibody (#115-065-072, Jackson ImmunoResearch) coupled to APC-streptavidin (#405207, Biolegend) were used for the staining. T cell infiltration data is represented as number of CD3-positive cells or CD3-positive-CAR-positive cells per mg of tumor or per μ L of blood.

Animal work was performed according to protocols approved by the Ethical Committee for the Use of Experimental Animals of the Vall d'Hebron Research Institute.

Immunohistochemical analysis of HER2 and p95HER2 expression

Tumor samples were fixed in 4% formaldehyde buffered to pH7 (stabilized with methanol) for 24 h and were then formalin-fixed and paraffin-embedded (FFPE). Fixed tissue samples were sectioned at 4 μ m thickness, heated at 60 °C, deparaffinized with xylene, and immunostained with anti-p95HER2 (32H2) antibody described in ref. 7 and with anti-HER2 (#A0485, Agilent Technologies). Next, the slides were incubated with EnVision System-HRP labeled polymer anti-mouse secondary antibody (#K4000, Agilent Technologies). Samples were then stained with DAB substrate chromogen (#K3468, Agilent Technologies) for 1–4 min and counterstained with harris hematoxylin

(#H3404, VectorLaboratories) for 2 min, followed by dehydration with ethanol and xylene, and finally mounted in DPX (#06522, Sigma-Aldrich).

TECH2 binding assays

HEK293T cells were infected with the same retrovirus used to transduce T cells expressing the different TECH2 constructs separated by a T2A with eGFP fluorescent protein. After confirming a transduction efficiency > 90%, HEK293T cells expressing the different TECH2s were plated in cell culture plates. Supernatant containing TECH2 was collected at confluence and used to stain different cell lines. For detection, a secondary anti-6x-His Tag Monoclonal Antibody conjugated with AF488 (#MA1-135-A488, Thermo Fisher Scientific) was used.

The supernatants of these cells were western blotted. Proteins were separated in an SDS-PAGE and transferred to a 0.45 µm nitrocellulose membrane (#10600002, GE Healthcare Biosciences) using the Trans-Blot (BioRad). The membrane was blocked with 5% non-fat dry milk in TBS-T (1× tris-buffered saline with 0.1% tween 20 (#P7949, Sigma-Aldrich)) and stained overnight with anti-6x-His Tag Monoclonal antibody conjugated with HRP (#MA1-135-HRP, Thermo Fisher Scientific). The membrane was washed three times, developed with Immobilon Chemiluminescence HRP Substrate (#WBKLS0500, Merck) and protein bands were visualized in AmershamTM Imager 600 (GE Life Sciences).

Quantification of TECH2Me

T cells expressing p95HER2.CAR-TECH2Me or untransduced vector (UTD) were counted and plated at 0.2×10^6 CAR-positive T cells/mL and let expand for 12 days in the presence of 300 IU/mL IL-2. At days 0, 4 and 12, supernatant was collected and TECH2Me levels secreted into the media were measured by competitive his-tag ELISA (# L00436, GenScript), by detecting the his-tag contained in the TECH2 constructs.

For in vivo half-life determination of TECH2Me, 600 ng of highly purified TECH2Me synthesized by GenScript (Rijswijk, Netherlands), were injected intravenously into NSG mice. At the indicated times, blood was withdrawn and serum was separated using clotting-gel (Z-Gel) tubes (#41.1378.005, Sarstedt) and spined at 10,000 × g for 5 min. Serum was then used for quantifying TECH2Me using competitive his-tag ELISA (#L00436, GenScript).

Metastasis assays

For lung metastases, MCF7 p95HER2 (1×10^6) or PDX433 cells (1×10^6) transduced with lentiviral vector pLENTI-CMV-V5-Luc Blast to express luciferase were injected in the tail vein of NSG mice, and after 1 month tumor cells colonized the lungs. To mimic brain metastases, MCF7 p95HER2 expressing luciferase cells (5×10^5) were injected intracranially in NSG mice. Mice with MCF7 p95HER2 cells were maintained with doxycycline treatment (1 g/L) in drinking water for inducing p95HER2 expression. All mice were treated intravenously with 3×10^6 CAR T cells twice. Tumor growth was monitored via bioluminescence imaging using the IVIS-200 Imaging System from Xenogen (PerkinElmer) upon luciferin administration (#E-1605, Promega).

Statistics

Data are represented as average ± standard deviation (SD), and the statistical analysis used is indicated in each figure legend. For in vitro experiments, two-sided Student's *t*-test using Excel, or two-way analysis of the variance (ANOVA) with Bonferroni correction for multiple comparisons using GraphPad Prism were performed. For in vivo experiments, mice were allocated randomly in treatment groups, with randomization performed manually to ensure that group means were balanced. Tumor growth curves were compared using two-way ANOVA with Bonferroni correction for multiple comparisons.

Statistical significance was defined as a *p*-value < 0.05. Unless otherwise specified, *p*-values indicated in the figures correspond to the comparison of each group (indicated by color) with the UTD or corresponding control group. Non-significant *p*-values are not shown. Efforts were made to reduce the number of animals used in the experiments.

Reporting summary

Further information on research design is available in the Nature Portfolio Reporting Summary linked to this article.

Data availability

All data associated with this study are included in the paper or its Supplementary Information file. All materials will be made available for the scientific community. Source data are provided with this paper.

References

- Ellerman, D. Bispecific T-cell engagers_ towards understanding variables influencing the in vitro potency and tumor selectivity and their modulation to enhance their efficacy and safety. *Methods* **154**, 102–117 (2019).
- Waldman, A. D., Fritz, J. M. & Lenardo, M. J. A guide to cancer immunotherapy: from T cell basic science to clinical practice. *Nat. Rev. Immunol.* **20**, 651–668 (2020).
- June, C. H. & Sadelain, M. Chimeric antigen receptor therapy. *N. Engl. J. Med.* **379**, 64–73 (2018).
- Arribas, J., Baselga, J., Pedersen, K. & Parra-Palau, J. L. p95HER2 and breast cancer. *Cancer Res.* **71**, 1515–1519 (2011).
- Scaltriti, M. et al. Expression of p95HER2, a truncated form of the HER2 receptor, and response to anti-HER2 therapies in breast cancer. *J. Natl. Cancer Inst.* **99**, 628–638 (2007).
- Parra-Palau, J. L. et al. Effect of p95HER2/611CTF on the response to trastuzumab and chemotherapy. *J. Natl. Cancer Inst.* **106**, 739 (2014).
- Parra-Palau, J. L. et al. A major role of p95/611-CTF, a carboxy-terminal fragment of HER2, in the down-modulation of the estrogen receptor in HER2-positive breast cancers. *Cancer Res.* **70**, 8537–8546 (2010).
- Sperinde, J. et al. Quantitation of p95HER2 in paraffin sections by using a p95-specific antibody and correlation with outcome in a cohort of trastuzumab-treated breast cancer patients. *Clin. Cancer Res.: Off. J. Am. Assoc. Cancer Res.* **16**, 4226–4235 (2010).
- Dorraj, E. et al. Development of a high-affinity antibody against the tumor-specific and hyperactive 611-p95HER2 isoform. *Cancers* **14**, 4859 (2022).
- Ruiz, I. R. et al. p95HER2-T cell bispecific antibody for breast cancer treatment. *Sci. Transl. Med.* **10**, eaat1445 (2018).
- Choi, B. D. et al. CAR-T cells secreting BiTEs circumvent antigen escape without detectable toxicity. *Nat. Publ. Group* **37**, 1049–1058 (2019).
- Madsen, L. et al. The tissue-specific rep8/UBXD6 tethers p97 to the endoplasmic reticulum membrane for degradation of misfolded proteins. *Plos One* **6**, e25061 (2011).
- Duro-Sánchez, S. et al. Therapy-induced senescence enhances the efficacy of HER2-targeted antibody–drug conjugates in breast cancer. *Cancer Res.* **82**, 4670–4679 (2022).
- Carter, P. et al. Humanization of an anti-p185HER2 antibody for human cancer therapy. *Proc. Natl. Acad. Sci. USA* **89**, 4285–4289 (1992).
- Liu, X. et al. Affinity-tuned ErbB2 or EGFR chimeric antigen receptor T cells exhibit an increased therapeutic index against tumors in mice. *Cancer Res.* **75**, 3596–3607 (2015).
- Goebeler, M.-E. & Bargou, R. C. T cell-engaging therapies - BiTEs and beyond. *Nat. Rev. Clin. Oncol.* **16**, 2825–434 (2020).
- Satoh, T. et al. Lapatinib plus paclitaxel versus paclitaxel alone in the second-line treatment of HER2-amplified advanced gastric

- cancer in Asian populations: TyTAN—a randomized, phase III study. *J. Clin. Oncol.* **32**, 2039–2049 (2014).
18. Thuss-Patience, P. C. et al. Trastuzumab emtansine versus taxane use for previously treated HER2-positive locally advanced or metastatic gastric or gastro-oesophageal junction adenocarcinoma (GATSBY): an international randomised, open-label, adaptive, phase 2/3 study. *Lancet Oncol.* **18**, 640–653 (2017).
 19. Tabernero, J. et al. Pertuzumab plus trastuzumab and chemotherapy for HER2-positive metastatic gastric or gastro-oesophageal junction cancer (JACOB): final analysis of a double-blind, randomised, placebo-controlled phase 3 study. *Lancet Oncol.* **19**, 1372–1384 (2018).
 20. Martínez-Sáez, O. & Prat, A. Current and future management of HER2-positive metastatic breast cancer. *Jco Oncol. Pr.* **17**, 594–604 (2021).
 21. Swain, S. M., Shastry, M. & Hamilton, E. Targeting HER2-positive breast cancer: advances and future directions. *Nat. Rev. Drug Discov.* **22**, 101–126 (2023).
 22. Morgan, R. A. et al. Case report of a serious adverse event following the administration of T cells transduced with a chimeric antigen receptor recognizing ERBB2. *Mol. Ther.* **18**, 843–851 (2009).
 23. Scaltriti, M. et al. Lapatinib, a HER2 tyrosine kinase inhibitor, induces stabilization and accumulation of HER2 and potentiates trastuzumab-dependent cell cytotoxicity. *Oncogene* **28**, 803–814 (2009).
 24. Tucker, D. F. et al. Isolation of state-dependent monoclonal antibodies against the 12-transmembrane domain glucose transporter 4 using virus-like particles. *Proc. Natl Acad. Sci. USA* **115**, E4990–E4999 (2018).
 25. Arenas, E. J. et al. Acquired cancer cell resistance to T cell bispecific antibodies and CAR T targeting HER2 through JAK2 down-modulation. *Nat. Commun.* **12**, 1237 (2021).

Acknowledgements

M.R.A. was supported by Secretaria d'Universitats i Recerca del Departament d'Empresa i Coneixement de la Generalitat de Catalunya (AGAUR-FI-DGR to M.R.A.). A.G.-E. received the support of a fellowship from the Predoctoral fellowship INPhINIT “la Caixa” Programme by “la Caixa” Foundation (LCF/BQ/DI21/118600412021 to A.G.-E.). S.D.-S. acknowledges the Spanish Ministerio de Universidades for a Formación de Profesorado Universitario grant (FPU20/05388 to S.D.-S.). J.A. acknowledges the financial support for this study from the Fundación Científica de la Asociación Española contra el Cáncer (FCAECC) (GCAEC19017ARRI and INNOV235333ARRI to J.A.) and the AECC EXCELLENCE ADVANCED THERAPIES ACCELERATOR PROGRAM (EPAEC222644VHIO to VHIO). In addition, this work has received support from the EU/EFPIA/Innovative Medicines Initiative 2 Joint Undertaking Immune-Image grant (831514 to J.A.). This study was also partially supported by a grant from the Breast Cancer Research Foundation (BCRF-21-008 to J.A.), by the Instituto de Salud Carlos III (ISCIII), co-funded by the European Union, through the projects CB16/12/00449, PMP22/00054 and PI19/01181 (to J.A.), and by the Comprehensive Program of Cancer Immunotherapy & Immunology II (CAIMI-II), supported by the BBVA Foundation (grant 53/2021 to J.A.). VHIO would like to acknowledge the State Agency for Research (Agencia Estatal de Investigación) for the financial support as a Center of Excellence Severo Ochoa (CEX2020-001024-S/AEI/10.13039/501100011033 to VHIO), the Cellex Foundation for providing research facilities and equipment, and the CERCA Programme from the Generalitat de Catalunya for their support of this research.

Author contributions

M.R.A. designed and performed most experiments, interpreted the data, and revised the manuscript. A.G.-E., S.D.-S. and I.R.-R., designed,

conducted, and interpreted some experiments and revised the manuscript. M.B.-B. and J.G., conducted some experiments. M.E., S.M.-M. and S.P.-R., performed IHC and performed some in vivo experiments. M.E.-B., V.P., S.E.-d.-R. and C.S. provided clinical advice and breast cancer patient samples. L.F. and L.S. performed intracranial injection into NSG mice. V.N., I.B., V.G., S.M.-L., E.G. provided relevant support at different stages of the project. E.M. and C.K. performed the humanization of p95HER2 scFv sequences. J. A. designed, acquired funding and supervised the study, interpreted the data, and wrote the manuscript.

Competing interests

J.A. has received research funds from Roche, Byondis, Menarini and Molecular Partners and consultancy honoraria from Menarini, Mnemo and ARKIN. J.A. is an inventor of patent applications EP22382294, EP20382457, EP16191933.7, EP0930183.5 and P200801652. M.R.A., I.R.-R., C.K., E.M., are inventors of patent application EP20382457. M.R.A., S.D., A.G.-E., I.R.-R., V.N. are inventors of patent application EP22382294. C.K. declares employment, patents and stock ownership with Roche. E.M. declares employment with Roche. E.G. reports: research agreements with Novartis, Roche, Thermo Fisher, AstraZeneca, Taiho, BeiGene, Janssen; consultant/advisor at Roche, Ellipses Pharma, Boehringer Ingelheim, Janssen Global Services, Seattle Genetics, Thermo Fisher, MabDiscovery, Anaveon, F-Star Therapeutics, Hengrui, Sanofi, Incyte; and payment or honoraria for speakers' bureaus from Merck Sharp & Dohme, Roche, Thermo Fisher, Lilly, Novartis, SeaGen. The remaining authors declare no competing interests.

Additional information

Supplementary information The online version contains supplementary material available at <https://doi.org/10.1038/s41467-024-53265-7>.

Correspondence and requests for materials should be addressed to Joaquín. Arribas.

Peer review information *Nature Communications* thanks Sebastian Kobold, Massimiliano Mazza and Alberto Zambelli for their contribution to the peer review of this work. A peer review file is available.

Reprints and permissions information is available at <http://www.nature.com/reprints>

Publisher's note Springer Nature remains neutral with regard to jurisdictional claims in published maps and institutional affiliations.

Open Access This article is licensed under a Creative Commons Attribution-NonCommercial-NoDerivatives 4.0 International License, which permits any non-commercial use, sharing, distribution and reproduction in any medium or format, as long as you give appropriate credit to the original author(s) and the source, provide a link to the Creative Commons licence, and indicate if you modified the licensed material. You do not have permission under this licence to share adapted material derived from this article or parts of it. The images or other third party material in this article are included in the article's Creative Commons licence, unless indicated otherwise in a credit line to the material. If material is not included in the article's Creative Commons licence and your intended use is not permitted by statutory regulation or exceeds the permitted use, you will need to obtain permission directly from the copyright holder. To view a copy of this licence, visit <http://creativecommons.org/licenses/by-nc-nd/4.0/>.

© The Author(s) 2024